Haptic Rendering involving an Elastic Tube for Assembly Simulations*

Qi Luo and Jing Xiao
IMI Lab, Department of Computer Science
University of North Carolina - Charlotte
Charlotte, NC 28223, USA
{*qluo, xiao*}*@uncc.edu*

***Abstract*— While there is considerable research on automatic assembly and virtual assembly of rigid parts, much less research is focused on assembly tasks involving deformable parts such as tubes, wires or deformable tools, etc. In this paper, we present a novel approach for simulating the behavior of the elastic tube via haptics during virtual assembly and modeling contact forces with high-fidelity and high rendering update rate by using the physical beam-bending model. The contact force is modeled based on different types of contact states with the effects of deformation and friction taken into account. Compliant motion is also simulated accordingly. We further test the virtual assembly method by implementing a specific assembly task and shows how such a virtual assembly environment can be used to conduct feasibility analysis of assembly motion plans to facilitate real-world automatic assembly.**

***Index Terms*— haptic rendering, contact state, elastic tube, virtual assembly, assembly planning, compliant motion.**

I. INTRODUCTION

Haptic devices allow a human user to interact with physical objects in a virtual environment simulated in a computer and to feel the simulated tactile feedback. With the advancement of such devices, an attractive area of application is virtual prototyping of manufacturing tasks. For example, a designer could test the design of assembly parts and assembly process by performing high-fidelity virtual assembly as if working with the actual physical parts in order to obtain important feedback rapidly for design improvement.

A typical assembly operation means a held part (by an operator) is moved to achieve a mating configuration with another part or subassembly. For high-precision or low-tolerance assembly operations, the effect of inevitable uncertainties becomes significant and manifest to various kinds of collisions or contact states between the held part and the environment. Thus, to simulate realistically such an operation in a virtual environment where a human operator holds a virtual part via a haptic device to perform the assembly, it is crucial to simulate the contact force and moment with models of high physical fidelity, and, at the same time, achieve a very high rendering update rate in kHz. How to achieve the often conflicting requirements of high physical fidelity and high rendering update rate is the major challenge of virtual assembly.

While there is considerable research on automatic assembly of rigid parts, and more recently, on virtual assembly of rigid parts (e.g., [1], [2]), much less research is focused on assembly tasks involving deformable parts such as tubes, wires or deformable tools, etc, which are often more complicated than assembly tasks with only rigid parts. Among the few papers about assembly tasks involving deformable parts, in [3] and [4], contact states and state transitions for assembly involving flexible hoses or deformable thin objects were addressed, which are helpful on creating robust manipulation routines in deformable object assembly tasks. In [5], [6] and [7], physically-based models (mass-spring model, FEM model or dual mechanical model) were presented to simulate the physical properties of deformable cables or flexible hoses, low computational costs and visually satisfying object behaviors were achieved in their virtual assembly simulations. However, the update rates of the models were at most around $20 \sim 30$Hz, which cannot satisfy the k Hz requirement on update rate for haptic rendering. There is little literature on haptics-based virtual assembly involving deformable objects.

In this paper, we study assembly operations involving an elastic tube and present a method of virtual assembly via haptics to simulate such operations. Our method achieves both high-fidelity and high rendering update rate of simulation by using the physical 'beam-bending' model to simulate the behavior of the elastic tube during assembly and modeling contact forces based on different types of contact states with the effects of deformation and friction taken into account. Compliant motion is also simulated accordingly. We further test the virtual assembly method by implementing a specific assembly task and shows how such a virtual assembly environment can be used to conduct feasibility analysis of assembly motion plans to facilitate real-world automatic assembly.

The paper is organized as follows. In Section II, we introduce general notations and assumptions. In Section III, we describe how to model and represent different contact states involving an elastic tube. In section IV, we present the physics-based deformation model and the corresponding contact force model for haptic and graphic simulation and rendering. In Section V, we describe the implementation of our method and present a specific example of assembly, and we discuss how to evaluate the feasibility of assembly motion plans with the same example using the virtual assembly environment. We conclude the paper in Section VI.

*This work is partially supported by the National Science Foundation Grants EIA-0224423 and IIS-0328782.

II. Assumptions and General Notations

We restrict our study in this paper to the elastic object scenarios as specified below.

A. Homogeneous isotropic linear elastic material

Depending on material properties, deformable objects can be categorized into many types [8]. In this paper, we focus on modeling deformable object that is made of homogeneous isotropic linear elastic material. This is a very commonly studied class of deformable objects in mechanics since the class covers a lot of materials including metals and certain composite materials.

B. Elastic tubes with only bending behavior

In [7], it is mentioned that the qualitative analysis of the deformation behavior has shown that under the magnitude of forces that could be applied manually during the operation, elastic tubes (e.g. steel flexible hoses, plastic hoses, aluminum soft tubes, rubber tube, etc) could be considered as torsionally rigid as well as rigid under tension and compression load cases. The deformation model is mainly characterized by a bending behavior.

C. Other physical properties

For an elastic tube, we assume that it has evenly distributed stiffness with a constant stiffness coefficient K and evenly distributed contact pressure. We use Coulomb friction with the static friction coefficient μ and kinetic friction coefficient μ_D. To simplify the case, we assume the gravity force of the elastic tube itself is much smaller than the react bending forces (i.e, thin shell tubes), and therefore the gravity force effect is neglected.

D. Force from the human operator

We assume that when a human operator holds an end of an elastic tube, the force exerted to the elastic tube is applied to the center of the held end of the tube.

III. Contact State Representation Involving an Elastic Tube

A. Review: representation of contact states between rigid objects

The notion of *principal contacts* (PCs) were first introduced to describe contact primitives between two rigid polyhedral objects in terms of the surface elements in contact [9]. A surface element can be a face (F), an edge (E), or a vertex (V). A face's boundary elements are the edges and vertices bounding it, and an edge's boundary elements are the vertices bounding it. Formally, a PC denotes the contact between a pair of surface elements that are not boundary elements of other contacting surface elements. This ensures that PCs are the highest level contact primitives to describe a contact state. For example, a face-face contact between two polyhedral objects is described just as a single face-face PC rather than in terms of a set of vertex-face or edge-face contacts. Each PC defines a single contact region of a point, a straight-line segment, or a planar region.

PCs were further extended to describe contact primitives for rigid non-polyhedral objects [10], where a surface element can again be a face, an edge, and a vertex. A face is a smooth surface or surface patch. An edge is a smooth intersection curve of two faces, which can be described either parametrically or as satisfying both implicit surface equations of the two faces. A vertex is either an apex of a surface (such as a cone) or an intersection point of two or more edges.

Built on the notion of PCs, a general topological contact state between two rigid objects is defined as a *contact formation* (CF) consisting of the set of PCs formed.

B. Representation of contact states involving an elastic tube

Contact states involving deformable objects are generally more varied and complicated than those between rigid objects. Some new contact states which cannot happen for rigid objects are possible if one of the objects is deformable. For example, Fig. 1a shows a contact state that is not possible if the tube-like object is not deformable. Moreover, the contact state representation for rigid objects is unable to tell whether a deformable object actually deforms in a contact state or not and how a deformation happens. As shown in Fig. 1b, the two contact cases cannot be distinguished if the contact state representation does not explicitly indicate deformation; however, the two states are different and should be distinguished.

Thus, contact state representation for rigid objects cannot be used directly to describe contact states involving deformable objects. Information regarding deformation has to be included in a contact state representation for contacts involving deformable objects. How to represent properly a contact state involving general deformable objects (which can be bent, compressed/expanded or even twisted) may not be a trivial problem. In this paper, however, we focus on representing contact states between an elastic tube and a rigid object, which can be done by extending the notion of PCs and CFs for contact states between rigid objects with some modifications.

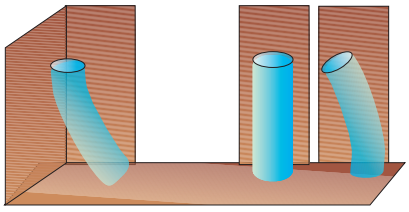

(a) (b)

Fig. 1. Examples of contact states involving a deformable tube:
(a) a contact state that is impossible if the tube does not deform;
(b) two contact states that cannot be distinguished if deformation is not indicated.

We extend the notions of PCs by introducing new symbols to indicate (1) deformation of the elastic tube and (2) how the deformation occurs with respect to a contact between the tube and the rigid object, i.e., the relative bending direction, since such information characterizes physical properties that can be different from one contact state to another. Let U_A and U_B

indicate two surface elements of the elastic tube A and the rigid object B respectively, and each element can be a face (F), an edge (E), or a vertex (V) in particular. We now add new symbols to the expression of a PC between U_A and U_B:

- If U_A and U_B are in contact while A does not bend, the PC between U_A and U_B is indicated as U_A–U_B (just as in the case of contacting rigid objects).
- If U_A and U_B are in contact while A bends but U_A does not deform, the PC between U_A and U_B is indicated as $\tilde{U_A}$–U_B.
- If U_A and U_B are in contact while U_A deforms, and if the concave side of U_A contacts U_B, the PC between U_A and U_B is indicated as $\tilde{U_A}\smile U_B$ (as in Fig. 2a); otherwise, if the convex side of U_A contacts U_B, the PC between U_A and U_B is indicated as $\tilde{U_A}\frown U_B$ (as in Fig. 2b).

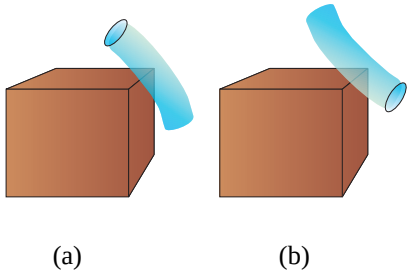

(a) (b)

Fig. 2. Examples of contact states representations w.r.t. deformation directions:
(a) contact involving the concave side of the deformed element: $\tilde{F_A}\smile E_B$
(b) contact involving the convex side of the deformed element: $\tilde{F_A}\frown E_B$.

Now with the added information, there are more types of PCs between an elastic tube and a rigid object than those between a rigid tube and another rigid object, as shown in Fig 3. Consequently, the types of CFs between an elastic tube and a rigid object are also more than those between a rigid tube and another rigid object.

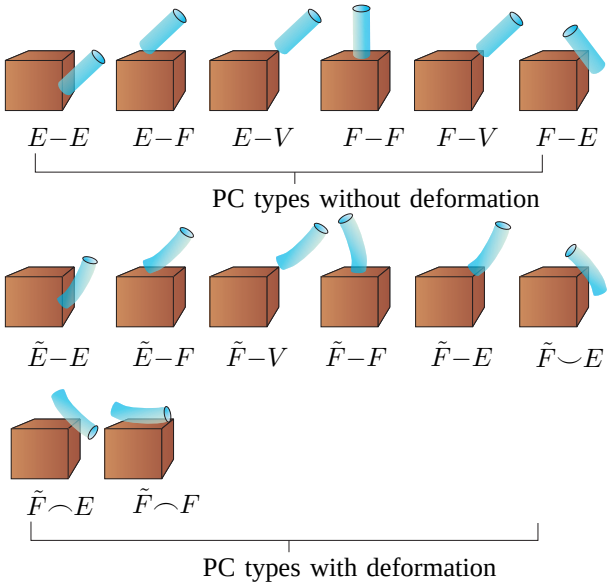

Fig. 3. Possible PC types involving an elastic tube and a rigid object

IV. Haptic Rendering of Contacts Involving an Elastic Tube

We first introduce how to model the deformation of an elastic tube with only bending behavior with the physics-based 'bending beam' model and then describe how to simulate the contact force and deformation shape change for haptic and graphic rendering.

A. Bending model

Now we describe how deformation is computed based on the Bernoulli-Euler bending beam theory [11] for an elastic tube with outer radius r_1, inner radius r_2, and length l (which are determined based on the undeformed shape of the elastic tube). Assume that the tube bends at one end with the other end held by an operator. Establish the tube coordinate system as O-xyz as shown in Fig. 4, where the origin is set at the center point of the held end of the tube, and the z axis is along the central line of the tube before it is bent and pointing to the other end of the tube. The x axis is along the bending force direction, and the y axis is orthogonal to both the z and x axes following the right-handed rule. A point p on the tube before it is bent has coordinates (x, y, z). Once the tube is pressed by a force F_x at the end where $z = l$, the tube bends, and the new coordinates of p is (x', y', z') satisfying

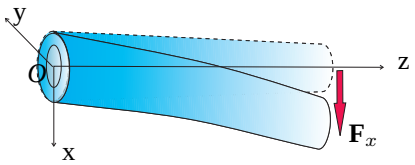

Fig. 4. Schematic of tube bending

$$
\begin{aligned}
x' &= \tfrac{1}{E}\tfrac{F_x}{I_y}[z^2(\tfrac{l}{2}-\tfrac{1}{6}z)+\tfrac{\nu}{2}(x^2-y^2)(l-z)] \\
y' &= \tfrac{\nu}{E}\tfrac{F_x}{I_y}xy(l-z) \\
z' &= z+\tfrac{1}{E}\tfrac{F_x}{I_y}[-\tfrac{1}{4}(x^3-xy^2) \\
&+\tfrac{3+2\nu}{4}(r_1^2+r_2^2)x+\tfrac{3+2\nu}{4}r_1^2r_2^2\tfrac{x}{x^2+y^2}-xz(l-\tfrac{1}{2}z)]
\end{aligned}
\tag{1}
$$

where E is the Young's modules, ν is Poisson's ratio and I_y is moment of inertia with respect to the y axis. At the end of the tube where $z = l$, the relation between the external force F_x normally applied to the end and the deformation displacement Δx of the end center $(0, 0, l)$ is

$$
F_x = \frac{3EI_y}{l^3}\Delta x \tag{2}
$$

B. Contact force simulation

When the end of the tube where $z = l$ contacts a rigid object to form a PC, the contact force can make the tube bend. To determine how the tube bends, we need to know the force $\mathbf{F}_x$ exerted on the elastic tube, which comes from the $\mathbf{F}_{sx}$ (component of the contact normal support force $\mathbf{F}_s$ along

the x axis of the tube) and $\mathbf{F}_{fx}$ (component of the tangential friction force $\mathbf{F}_f$ along the x axis of the tube), that is:

$$\mathbf{F}_x = \mathbf{F}_{sx} + \mathbf{F}_{fx} \tag{3}$$

Let $d < \epsilon$ denote the minimum distance between the corresponding contacting elements in the virtual PC, where $\varepsilon > 0$ is a small threshold. We model the contact normal force $\mathbf{F}_s$'s magnitude based on the spring model as:

$$||\mathbf{F}_s|| = K(\varepsilon - d) \tag{4}$$

where K is the stiffness coefficient. To prevent penetration, the constraint-based idea of a virtual proxy can also be used here [12]. Its direction is always normal to the tangent plane of the two contacting surface elements, which we call the contact plane.

For the friction force $\mathbf{F}_f$, since it can be either static or kinetic, we need to detect whether the elastic tube is stuck upon contact or performs a compliant motion tangentially along the contact surface of the rigid object. First, assume that the elastic tube is stuck at the current time step i due to the friction force from the rigid object $\mathbf{F}_f$. Since the tube coordinate system O-xyz can be tracked via the haptic device at any time, the deformation of the tube's contact end center along the x axis can be calculated as the distance Δx between the held end center to the contact end center of the tube along the current x-axis. Therefore, $\mathbf{F}_x$ can be computed from equation (2). Also, from the known $\mathbf{F}_s$'s direction and calculated magnitude from equation (4), its x-axis component $\mathbf{F}_{sx}$ can be obtained as the projection of $\mathbf{F}_s$ on the x-axis. Subsequently, $\mathbf{F}_{fx}$ can be calculated from equation (3). Let θ be the angle between x axis and the intersection line of the xz plane and the contact plane, $\mathbf{F}_f$ can be computed as

$$||\mathbf{F}_f|| = ||\mathbf{F}_{fx}||/\cos\theta \tag{5}$$

According to [13], the maximum static friction from objects of different elasticity is proportional to the contact normal force $||\mathbf{F}_s||^\beta$, $\frac{2}{3} \leq \beta \leq 1$, in the empirical equation $f_{max} = K||\mathbf{F}_s||^\beta$, where the coefficient K and β were given in [14] for various deformable materials. For an elastic solid, $\beta = \frac{2}{3}$.

Now if $\|\mathbf{F}_f\| \leq f_{max}$, our assumption is correct: the elastic tube is indeed stuck by the static friction so that it will not have a compliant motion at the current time step. The contact will not change the contact point or equivalent contact point p_c on the elastic tube [15](as shown in Fig. 5b). The total contact force response from the rigid object to the elastic tube is $\mathbf{F}_c = \mathbf{F}_s + \mathbf{F}_f$.

Otherwise, if $\|\mathbf{F}_f\| > f_{max}$, this represents an impossible case for static friction, indicating that our assumption that the elastic tube is stuck is incorrect. On the contrary, the elastic tube in fact makes a compliant motion. If the origin p_0 of the frame of the elastic tube has moved tangentially from time step $i-1$ to time step i with a distance Δd, then to model the effect of compliant motion, we also shift p_c the distance Δd to obtain its new position. Based on the new position of p_c, we re-compute the tangential deformation x' and then $\mathbf{F}_f$, which should satisfy $\|\mathbf{F}_f\| \leq f_{max}$. The total contact force response from the rigid object to the elastic tube is then $\mathbf{F}_c = \mathbf{F}_s + \mathbf{F}_f$.

Accordingly, there is a shift of the deformed shape of the elastic tube at time step i from that at time step $i-1$ due to compliant motion (as shown in Fig. 5c).

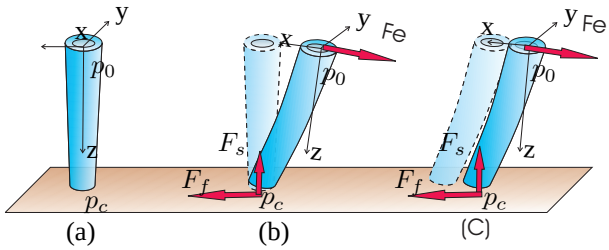

Fig. 5. The effect of contact friction (F_e is the exerted force):
(a) originally undeformed tube,
(b) $F_f \leq f_{max}$, the tube bends and is stuck,
(c) $F_f > f_{max}$, the tube bends and slides.

Above shows how to compute the contact force at a single-PC contact. If two or more PCs occur, by simply decomposing the tube into segments separated by the contact(s) on the side surface of the tube, the above force computing method can be applied to each segment i to compute the corresponding contact normal force $\mathbf{F}_{si}$ and friction force $\mathbf{F}_{fi}$, and the total contact force $\mathbf{F}_c$ for a n-PC CF can be achieved as

$$\mathbf{F_c} = \sum_{i=1}^{n} (\mathbf{F}_{si} + \mathbf{F}_{fi}) \tag{6}$$

For example, as shown in Fig. 6, one PC occurs at the end of the tube while the other PC occurs on the side surface of the tube. Now we can think of the whole tube as two separated segments: segment 1 is from the held end of the tube to the cross-section of the tube that goes through the contact point on the side surface, and segment 2 is the remaining part. Now for segment 1, its local frame O-$x_1y_1z_1$ is the same as the frame for the whole tube. The contact happens at the cross-section with the contact support force F_{s1} and friction force F_{f1}, which can be calculated by the same method for a single-PC CF. For segment 2, we view the cross-section as the held end. We can establish a local frame O-$x_2y_2z_2$ for segment 2 in the following way: the origin is set at the center of the cross-section, the z_2 axis is obtained by projecting z_1 along the normal direction of the cross-section, and the x_2 axis is along the projection of x_1 on the cross-section. For this segment, the contact happens at the end of the tube, and the contact support force F_{s2} and friction force F_{f2} can be calculated by the same method as in the case of a single-PC CF.

For graphic rendering of a deformed tube, since the elastic tube can be represented as a point mesh, the change on the position of any point on the tube can be easily calculated from (1), the shape of the deformed tube can therefore be rendered.

V. An Implemented Example of Virtual Assembly

We have implemented the method above for haptic and graphic rendering of contact states between an elastic tube and a rigid object in a virtual environment by a program in C++ on a personal computer with dual Intel Xeon 2.4GHz Processors and 1GB system RAM connected to a PHANToM

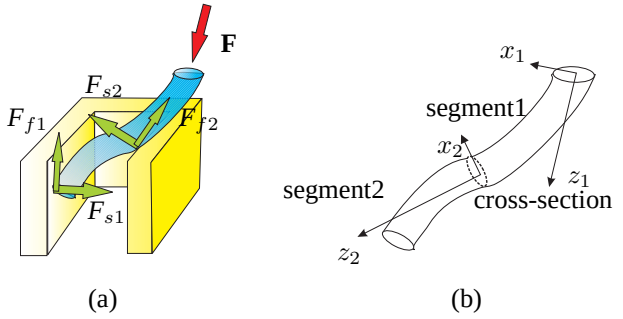

Fig. 6. Example of a 2-PC CF:
(a) contact forces;
(b) segmentation of the deformed tube into two parts

Premium 1.5/6DOF device. The human operator can virtually hold the elastic tube at one end via the haptic device and make any contact or compliant motion with respect to a rigid object.

Specifically, we have applied our method to a typical assembly task: inserting an elastic tube into a rigid guiding groove (see Fig. 7). Note that the groove could be closed, but we make it open so that contact states between the tube and the inside of the groove can be seen easily. We also exaggerate the clearance between the tube and the groove for the same purpose.

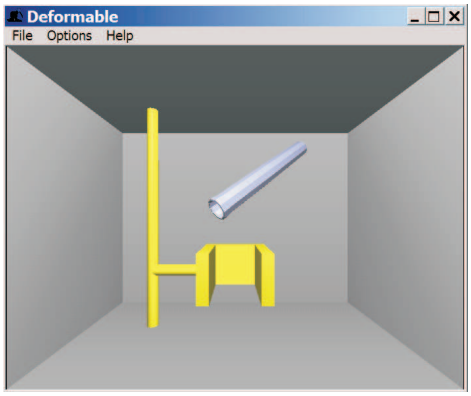

Fig. 7. An example assembly task

Table I lists the values of parameters used in our implementation, where m is the mass of the tube, and the rest of the parameters are introduced earlier in the paper.

TABLE I
PARAMETERS USED IN IMPLEMENTATION

P	Value	P	Value
$m(kg)$	1.0	$g(N/Kg)$	9.8
μ	0.7	μ_D	0.08
$K(N/mm)$	10	$\varepsilon(mm)$	1.0
$\rho(kg/m^2)$	1100 [a]	$E(N/m^2)$	$3 \cdot 10^6$ [a]
ν	0.5 [a]		

[a]Parameters of Rubber

In the following, we describe how our virtual assembly environment based on haptic rendering can serve as an excellent tool to evaluate different assembly motion plans involving the elastic tube, using the task of inserting the elastic tube into the rigid guiding groove as an example.

A. Contact state graph

A contact state graph represents all valid contact states and their neighboring relations between two objects. In the graph, each node denotes a contact state, and two neighboring contact states is indicated by the arc between the two corresponding nodes. Based on such knowledge, relative compliant motion or assembly motion can be planned as a sequence of contact state transitions connecting the starting state to the goal state. Hence, it is quite important to acquire the knowledge of a contact state graph. Work has been done on automatic generation of contact state graphs between rigid polyhedral objects [16].

In order to obtain assembly motion plans for the example task of inserting an elastic tube into a rigid groove, we also build a contact state graph based on the extended contact state representation introduced earlier (Section III.B). Fig. 8 shows the contact state subgraph consisting of the possible single-PC contact states between the elastic tube and the left side of the groove that occur during insertion. The contact state subgraph consists of the possible single-PC contact states between the elastic tube and the right side of the groove can be obtained in a similar fashion. Besides these two subgraphs, the complete contact state graph also consists of all possible multiple-PC contacts that involve both sides of the groove.

B. Heuristics for state transition

While there are many more contact states when an elastic tube is involved than the case with only rigid objects in contact, not all neighboring contact state transitions enumerated in a contact state graph involving the elastic tube are equally desirable in the insertion operation of the tube. Therefore, it is useful to study some state transition heuristics to reduce the number of state transitions and accordingly, the number of assembly motion plans (as sequences of state transitions).

Here we introduce a number of heuristics for preferred state transitions from one contact state to a neighboring contact state via a compliant motion of the elastic tube, taking into account friction and bending energy.

- The transition should minimize the friction force, i.e., it is preferred to change from a multi-PC contact state to a single-PC contact state in some cases.
- The transition should minimize the bending energy of the tube, i.e., the transition should avoid bending the tube as much as possible while keeping the tube in contact. A state transition that leads to reducing more bending energy is always preferred.
- The transition should minimize the motion distance towards the goal state.

Fig. 9 shows an example of a preferred state transition to minimize the friction as well as the bending energy.

After applying these heuristics, the numbers of state transitions for assembly motion plans can be much reduced, which

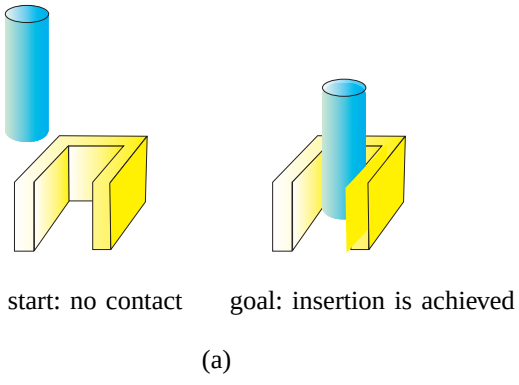

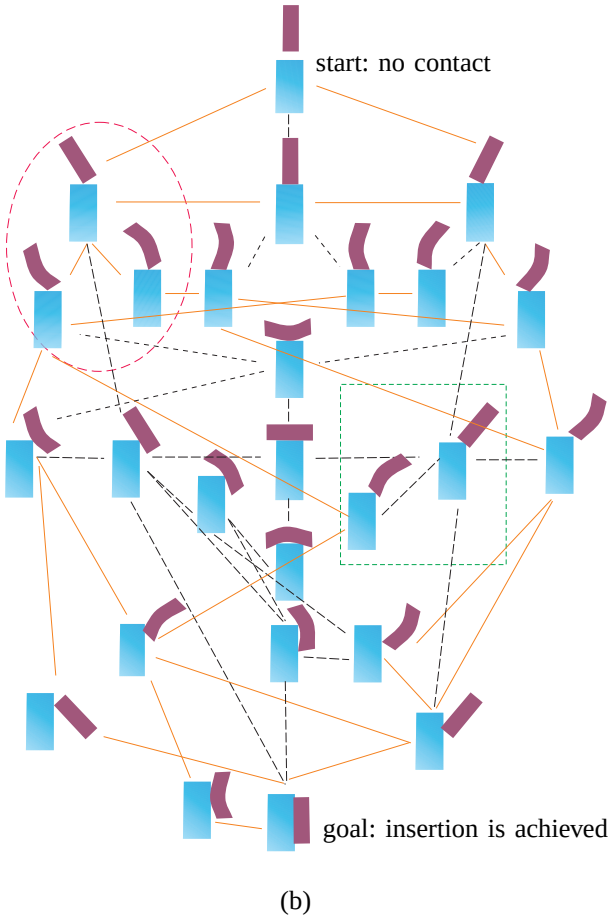

Fig. 8. Example of a contact state subgraph for a specific assembly task: (a) schematic of the assembly task of inserting an elastic tube into a rigid groove from the left side of the groove; (b) the contact state subgraph (note that the orange solid lines show simplified contact state graph after applying the transition rules described in Section V-B.)

means the number of possible contact states is much reduced, resulting in a simplified contact state graph, as shown in Fig. 8 with the connecting solid lines.

C. Evaluation of assembly motion plans

Although a simplified contact state graph can be obtained by applying the heuristics described, there are still some uncertain cases of state transition due to the deformation of the tube. At a contact state where it has more than one neighboring contact

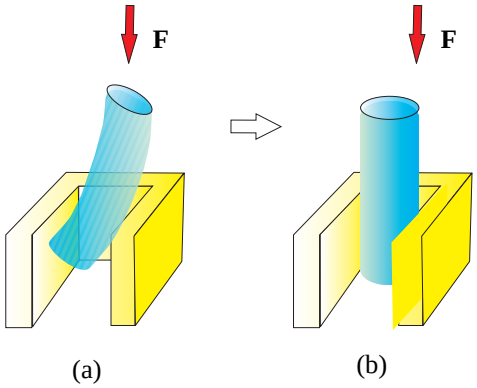

Fig. 9. An example of a preferred contact state transition

states (equally preferred based the heuristics introduced), it is not always clear the transition to which neighboring contact state is easier to achieve during the assembly operation. For example, inside the red circle in Fig. 8, there are two possible transitions for the top state node to its two neighboring nodes, but without knowing the exact strength and direction of the exerted force for transition, it is impossible to know which transition is better. In addition, some contact states shown in the contact state graph may or may not be feasible for assembly tasks with certain motion direction. (e.g. for the two contact states in the green square box in Fig. 8, it is impossible for transition from the top-right state node to the left-bottom one if the deformable tube is keep moving toward right).

By our introduced approach of high-fidelity virtual assembly based on haptic rendering, the above problems of ambiguity can be solved. A virtually fulfilled contact state transition means not only a feasible transition but also an easier transition generally. Feasible and highly robust assembly motion plans can be found and verified, impossible contact states or infeasible state transitions in a pre-built contact state graph can be eliminated, and missing contact states can be added.

Fig. 10 shows the snapshots of a feasible assembly motion sequence to achieve the example assembly task of inserting an elastic tube into a rigid guiding groove that we tested in our haptics-based virtual assembly environment.

VI. Conclusions

A novel approach has been proposed to represent contact states between an elastic tube and a rigid object and to simulate the contact force including friction with or without compliant motion between the tube and the other object as well as tube deformation due to contact for haptic rendering, which is based on beam bending theory and physics-based friction model involving deformable objects. Our approach avoid the drawbacks of low physical accuracy or time-consuming integration of the common mass-spring models or FEM models for deformable objects. Implementation shows that our method achieves both physical realism and real-time efficiency with an update rate of over 1 *k*Hz, including collision detection and rendering both haptic forces and graphic shape changes due to deformation. The paper also demonstrates its application to high-fidelity

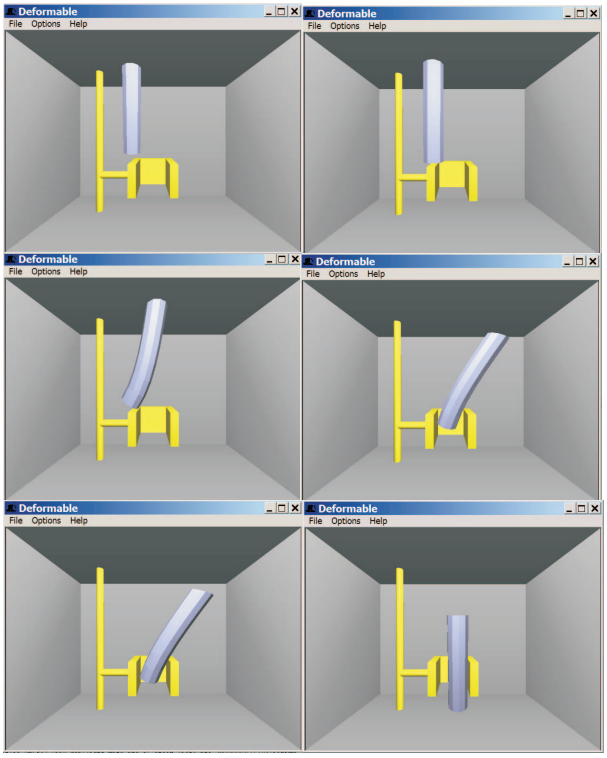

Fig. 10. Left-to-right, top-to-down: snapshots of the haptic and graphic rendering of a feasible assembly motion sequence for inserting the elastic tube into the rigid groove.

virtual assembly to enable effective evaluation of the feasibility and robustness of assembly motion plans.

The next step of this research is to extend the method to deal with more complicated deformable objects and contact situations and to further explore its application to finding both feasible and optimized motion plans for assembly tasks effectively.

REFERENCES

[1] G. Zachmann and A. Rettig, "Natural and robust interaction in virtual assembly simulation," in *The Proceedings of Eighth ISPE International Conference on Concurrent Engineering: Research and Applications ISPE/CE2001*, July 2001.

[2] Q. Luo and J. Xiao, "Physically accurate haptic rendering and virtual assembly," *Transactions of North America Manufacturing Research*, vol. 32, pp. 231–238, June 2004.

[3] D. Henrich, T. Ogasawara, and H. W¨rn, "Manipulating deformable linear objects contact states and point contacts -," in *1999 IEEE International Symposium on Assembly and Task Planning (ISATP'99)*, (Porto, Portugal), pp. 61–70, July 1999.

[4] H. Wakamatsu, R. Teramoto, A. Tsumaya, K. Shirase, and E. Arai, "Representation and planning of deformable thin object manipulation," in *Proceedings of the 4th International Conference on Machine Automation*, (Tampere, Finland), pp. 419–426, 2002.

[5] A. L. und E. Schmer, "A virtual environment for interactive assembly simulation: From rigid bodies to deformable cables," in *5th World Multiconference on Systemics, Cybernetics and Informatics (SCI'01),Vol. 3 (Virtual Engineering and Emergent Computing)*, pp. 325–332, 2001.

[6] R. Rabaetje, "Real-time simulation of deformable objects for assembly simulations," in *Proceedings of the Fourth Australian user interface conference on User interfaces, Vol. 18*, pp. 57–64, 2003.

[7] J.-C. Léon, U. Gandiaga, and D. Dupont, "Modelling flexible parts for virtual reality assembly simulations which interact with their environment," in *Proc. of IEEE Int. Conf. on Shape Modeling and Applications*, (Genova, Italy), pp. 335–344, May 07-11 2001.

[8] B. Berenberg, "Dictionary of composite materials technology," in *http://composite.about.com/library/glossary/blglossary.htm*, Composites/Plastics Dictionary.

[9] J. Xiao, "Automatic determination of topological contacts in the presence of sensing uncertainties," in *Proceedings of the 1993 International Conference on Robotics and Automation*, May 1993.

[10] Q. Luo, E. Staffetti, and J. Xiao, "Representation of contact states between curved objects," in *Proc. of IEEE Int. Conf. on Robotics and Automation*, pp. 3589–3595, 2004.

[11] T. Belytschko, W. Liu, and B. Moran, *Nonlinear Finite Elements for Continua and Structures*. John Wiley and Sons LTD, 2000.

[12] D. Ruspini, K. Kolarov, and O. Khatib, "Haptic interaction in virtual environments," in *Proc. of IEEE International Conference on Intelligent Robots and Systems. (IROS)*, Sept. 1997.

[13] I. Brown, *Abrasion and Friction in Parallel-lay Rope Terminations*. Ph.D. thesis, University of Cambridge, UK, March 1997.

[14] H. Howell and J. Mazur, "Amonton's law and fiber friction," *Journal of the Textile Institute*, vol. 44, no. 2, 1953.

[15] Q. Luo and J. Xiao, "Physically accurate haptic rendering with dynamic effects," *IEEE Computer Graphics and Applications*, vol. 24, pp. 60–69, Nov/Dec 2004.

[16] J. Xiao and X. Ji, "On automatic generation of high-level contact state space," *The International Journal of Robotics Research*, vol. 20, pp. 584–606, July 2001.